QUANTUM DOT AS A MECHANISM TO SUPRESS CHARGE RECOMBINATION IN POLYMER SOLAR CELL

Genene Tessema Mola[a*] and Abiodun Kazeem Ogundele[a]

[a] *School of Chemistry & Physics, University of KwaZulu-Natal, Scottsville (South Africa)*

Abstract

Effective light trapping mechanisms in thin film polymer solar cells (PSC) are leveraged by employing group II-VI semiconductor quantum dots. Core-shell semiconductor quantum dots ($Cd_xS/Zn_{1-x}S$ SQD) were synthesised via the microwave irradiation method. The SQDs were incorporated into the electron transport layer of PTB7:PC71BM blend PSC to assist in light trapping and charge collection processes. The measured device parameters suggest that the inclusion of SQD has significantly enhanced the solar cell's power conversion efficiency (PCE) due to improved energy transfer, exciton generation, and charge collection processes in PSCs. Moreover, the performances of the solar cells are found to be dependent on the concentration of SQD in the transport layer. Hence, the best efficiency recorded was 7.13% at an optimal concentration of 0.375 wt.%, which is an increment in PCE by nearly 23%.

Keywords: Quantum Dots, Polymer Solar cell, Solar Energy,

10.18086/eurosun.2024.09.07 Available at http://proceedings.ises.org

1.1 Introduction

Solar energy remains one of the cleanest, and most desirable alternative sources of energy to replace those environmentally unfriendly yet depleted fossil fuels to reduce global greenhouse gases (Ritchie & Roser, 2023). A vast amount of solar energy, radiated from the Sun per hour could have been enough to fulfil the energy demand for the world population for a year, but unfortunately, it is under-utilized and accounts for only about 4.5% of global electricity generation today, according to the International Energy Agency (IEA). This is due to various reasons ranging from cumbersome manufacturing processes, high cost of solar cell fabrication, and knowledge gaps on renewable energy sources. Interestingly, organic solar cells (OSC) are cost-effective, lightweight, solution-processable and suitable for roll-to-roll production making them more attractive from an economic perspective with the power conversion efficiencies (PCEs) currently stands over 20%, which is comparable to several to inorganic solar cell technologies (Guo et al., 2023). However, OSCs still suffer from a shortfall in photons to energy conversion efficiencies because of inherent inadequacies and challenges like environmental instability, low charge transport properties, non-robust temperature tolerance, narrow absorption range, competitive market, facelift cost etc. (Li et al., 2019; Ma et al., 2020).

This study demonstrates the application of microwave-synthesised core-shell semiconductor quantum dot (SQD) ($Cd_xS/Zn_{1-x}S$) in the electron transport layer of an inverted thin film polymer solar cell (TFPSC) containing photo-active layer blends of poly[[4,8–bis[(2-ethylhexyl)oxy]benzo[1,2-b']dithiophene-2,6-diyl][3-fluoro-2-[(2-ethyl hexyl)-carbonyl]thieno[3,4-b]thiophenediyl]]:[6,6]-phenyl C_{71} butyric acid methyl ester (PTB7:PC71BM). The SQD materials ($Cd_xS/Zn_{1-x}S$) with medium energy bandgap core and wide bandgap shell were used in the electron transport layer of TFPSC to assist in improving light trapping in the medium. These combined effects of core-shell SQD can be used to broaden optical absorption spectra leading to high light trapping resulting in an improved solar cell performance.

1.2 Synthesis of Semiconductor Quantum Dots

The bottom-up synthesis method involving two precursors was employed here designed by Soltani *et al.*, Shi *et al.*, and Rafea *et al (Rafea et al., 2009; Shi et al., 2011; Soltani et al., 2012)* . The core-shell SQD was synthesised via a two-step path: synthesis of core (Cd_xS) followed by the shell's growth ($Zn_{1-x}S$). 1.33265 g of Cadmium acetate was dissolved in a beaker containing 100 mL of ethylene glycol to obtain 0.05 M, thiol-stabilized with 4 mL thioglycolic acid followed by addition of 0.56343 g (75 mmol) of thioacetamide. The reaction was allowed to stir for about 10 min at about 5000 rpm. The reaction was then transferred into Russel Hobbs (Model no. RHEM21L) domestic microwave with an output power of 700W, the reaction was made to follow a working cycle of 30% for 25 minutes. The second precursor was achieved via the same process with lower concentrations, 0.54873 g (25 mmol) of zinc acetate was dissolved in a beaker containing ethanol, stirred for ten minutes at a speed of 5000 rpm, and later transferred to a microwave oven following a similar working cycle used for the core precursor. The precursors were added dropwise and allowed to disperse uniformly using a sonication bath for 60 min at 40ºC. The final precipitates were cooled to room temperature and centrifuged for about 10 min at a speed of 4000 rpm. This was followed by re-dispersing in deionized water and ethanol several times to remove the excess ionic remnants. Eventually, the SQD was dried in a vacuum oven at 60ºC for 24 h and its morphology was later subjected to various characterisation techniques.

1.3 J-V Characteristics of the Devices

An inverted device architecture composed of different layers of materials shown in Fig. 1a is employed in the current investigation. The current density-voltage (J-V) characteristics data under illumination conditions were measured from the fabricated solar cells are provided in Table 1. The data clearly shows an increase in the measured photocurrent as the result of the inclusion of SQD in the charge transport layers at different concentrations. Furthermore, the performance of the devices is found to be dependent on the concentration of the SQD in the medium. The best device performance found was PCE = 6.62% at the concentration of 0.375 wt%. This is growth in PCE by nearly 16% compared to the reference cell. Furthermore, the influence SQD on charge generation/recombination processes were analysed using generated photocurrent (J_{ph}) and effective voltage (V_{eff}) as presented in Fig. 1d to deduce exciton dissociation efficiency, charge collection efficiency, and saturation current (J_{sat}). The latter was used to determine the maximum exciton generation ($G_{max} = J_{sat}/_{qL}$). The probabilities of charge dissociation (η_{diss}) and collection (η_{coll}) of the pristine and modified

devices were determined by evaluating ($^{J_{ph}}/_{J_{sat}}$) under short circuit and maximum power output area of the curve, respectively. The device with 0.375 wt.% exhibited the highest probability of dissociation and collection of charges with magnitude of 94.71% and 69.9%, respectively as provided in Table 2.

Table 1: The Thin film Polymer solar cells' parameters for devices with/without SQD devices in ETL

ZnO:/$Cd_xS/Zn_{1-x}S$	V_{oc} (V)	$J_{sc}\,(mAcm^{-2})$	FF (%)	PCE (%)	$R_s(\Omega)$	$R_{SH}\,(K\Omega)$
Pristine	0.69 ± 0.01	15.49 ± 0.18	52.59 ± 1.04	5.70 ± 0.08	291.5	8.78
0.125 wt.%	0.63 ± 0.01	17.90 ± 0.93	53.30 ± 1.04	6.62 ± 0.08	234.2	8.68
0.375 wt.%	0.65 ± 0.02	18.95 ± 0.55	54.62 ± 1.62	7.01 ± 0.12	229.2	8.82
0.625 wt.%	0.64 ± 0.04	14.33 ± 0.04	52.00 ± 1.43	4.81 ± 0.08	514.1	10.1

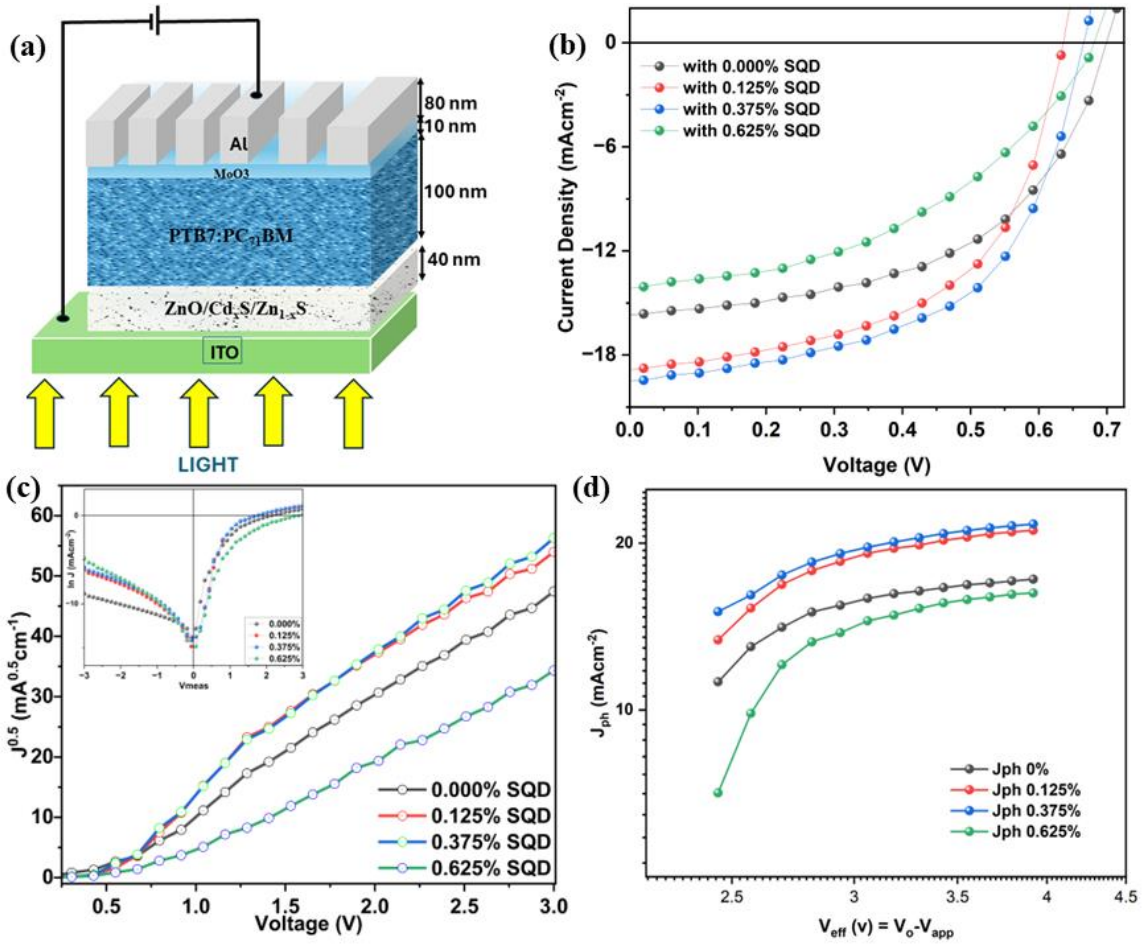

Fig. 1. (a) Inverted device architecture of PSC with modified ETL (b) J-V graphs under illumination & (c) $J^{0.5}$-V graphs under dark conditions (inset SCLC) (d) J_{ph} vs. V_{eff} for TFPSCs pristine and modified ETL devices.

Table 2: Charge transport parameters of TFPSCs w/wo SQD in electron transport layer

ZnO/$Cd_xS/Zn_{1-x}S$	$\mu_l(cm^2S^{-1}V^{-1})$	γ (cm V^{-1})	$G_{max}(m^{-3}s^{-1})$	η_{diss} (%)	η_{coll} (%)
Pristine	3.02×10^{-6}	-6.58×10^{-5}	1.08×10^{27}	85.9	66.1
0.125 wt.%	4.12×10^{-6}	-1.76×10^{-4}	1.32×10^{27}	89.3	66.9
0.375 wt.%	4.36×10^{-6}	-1.29×10^{-4}	1.35×10^{27}	94.7	70.0
0.625 wt.%	1.44×10^{-6}	-7.67×10^{-6}	1.02×10^{27}	87.8	62.1

Importantly, all SQD incorporated devices showed enhanced dissociation efficiency, underscoring the positive impacts of the SQD doped into the ETL buffer layer. On the other hand, the impact of SQD on the charge transport processes were investigated using the measured space charge limited current (SCLC) taken without the influence photons generated current. The Mutt-Gurney charge transport equation eq (1) is used to compare with the SCLC data to be able to derive the transport parameters. The low field mobility (μ_l), which is a

measure of charge carriers' movement in the TFPSCs under low electric field conditions and activation factor (γ) can be determined by an equation of the form:

$$J = {}^{9}/_{8}\ \varepsilon_o \varepsilon_r \mu_l\, {V^2}/_{L^3}\, e^{0.89\gamma\sqrt{{V}/{L}}}, \qquad (1)$$

where $\varepsilon_r = 3.5$ is the relative permittivity of PTB7:PC71B, ε_o is the permittivity of free space ($= 8.85 \times 10^{-12}\ m^{-3}kg^{-1}s^4A^2$), L(~ 150 nm) is the distance between the aluminium and ITO electrodes (see Fig 1a). The linear fittings of $J^{0.5}$ against V (obtained under dark conditions) as shown in Fig. 1c were eventually used to determine the values of the low field mobility for pristine devices and SQD-modified devices. The results of the analysis suggest that indeed the charge mobility in the medium has improved by a factor of 1.4 at the optimum SQD concentration in ETL compared to the reference cell.

4. Conclusion

Core-shell ternary semiconductor quantum dots ($Cd_xS/Zn_{1-x}S$) were employed as a mechanism for light trapping in an inverted TFPSC whose photoactive layer is composed of PTB7:PC71BM blend. The devices with the modified electron transport layer showed significant improvement in power conversion efficiency and device stability compared to the reference cell. The investigation results suggest that the improved device performances depend on SQD concentration in the ETL. The optimum SQD concentration for the best device performance recorded was 0.375 wt.%, which resulted in PCE of 7.01%, which is an increase of 23.4% compared to the reference cell. Such enhanced solar cell performance was attributed to the improved excitons generation, and effective light trapping in the absorber medium. This study showed the characteristic synergy inherent in semiconductor quantum dots in improving the various metrics of thin film polymer solar cells ultimately leading to better device parameters and environmental stability.

References

Guo, C., Fu, Y., Li, D., Wang, L., Zhou, B., Chen, C., Zhou, J., Sun, Y., Gan, Z., & Liu, D. (2023). A Polycrystalline Polymer Donor as Pre-Aggregate toward Ordered Molecular Aggregation for 19.3% Efficiency Binary Organic Solar Cells. *Advanced Materials*, *35*(41), 2304921.

Li, K., Wu, Y., Tang, Y., Pan, M. A., Ma, W., Fu, H., Zhan, C., & Yao, J. (2019). Ternary blended fullerene-free polymer solar cells with 16.5% efficiency enabled with a higher-LUMO-level acceptor to improve film morphology. *Advanced energy materials*, *9*(33), 1901728.

Ma, Q., Jia, Z., Meng, L., Zhang, J., Zhang, H., Huang, W., Yuan, J., Gao, F., Wan, Y., & Zhang, Z. (2020). Promoting charge separation resulting in ternary organic solar cells efficiency over 17.5%. *Nano Energy*, *78*, 105272.

Ogundele, A. K., & Mola, G. T. (2022). Ternary atoms alloy quantum dot assisted hole transport in thin film polymer solar cells. *Journal of Physics and Chemistry of Solids*, *171*, 110999.

Rafea, M. A., Farag, A., & Roushdy, N. (2009). Structural and optical characteristics of nano-sized structure of Zn0. 5Cd0. 5S thin films prepared by dip-coating method. *Journal of Alloys and Compounds*, *485*(1-2), 660-666.

Ritchie, H., & Roser, M. (2023). What are the safest and cleanest sources of energy? *Our World in Data*.

Shi, J., Liang, Z., Lu, X., Tong, Y., Su, C., & Liu, H. (2011). The roles of defect states in photoelectric and photocatalytic processes for Zn x Cd 1− x S. *Energy & Environmental Science*, *4*(2), 466-470.

Soltani, N., Saion, E., Erfani, M., Bahrami, A., Navaseri, M., Rezaee, K., & Hussein, M. Z. (2012). FACILE SYNTHESIS OF ZnS/CdS AND CdS/ZnS CORE-SHELL NANOPARTICLES USING MICROWAVE IRRADIATION AND THEIR OPTICAL PROPERTIES. *Chalcogenide Letters*, *9*(9).

Xia, Y., Nguyen, T. D., Yang, M., Lee, B., Santos, A., Podsiadlo, P., Tang, Z., Glotzer, S. C., & Kotov, N. A. (2011). Self-assembly of self-limiting monodisperse supraparticles from polydisperse nanoparticles. *Nature nanotechnology*, *6*(9), 580-587.

Zhou, P., Lan, W., Gu, J., Zhao, M., Wang, Z., Liao, Y., Liu, Y., Pu, H., Ding, J., & Wei, B. (2020). High-efficiency organic photovoltaic cells with an antimony quantum sheet modified hole extraction layer. *IEEE Journal of Photovoltaics*, *11*(1), 111-117.